OPEN ACCESS
Journal of Multidisciplinary Applied Natural Science Vol. xx No. xx (xxxx) https://doi.org/10.47352/jmans.2774-3047.289
Check for updates
Research Article

Preparation and Characterization of Cellulose-clay Composite using Indonesian Natural Bentonite for Cr(VI) Adsorption

Julinawati Julinawati*, Eka Nadia, Irfan Mustafa, and Suryati Suryati

Received : February 6, 2025	Revised : June 20, 2025	Accepted : June 28, 2025	Online : August 6, 2025

Abstract
Contamination of Cr(VI) is of global concern, whereas the innovation in wastewater treatment is required. Combination of bentonite and cellulose could produce an effective adsorbent to treat Cr(VI)-containing wastewater. The aim of this study was to investigate the use of composite bentonite/cellulose (B/Cell) to remove Cr(VI) in the aqueous media, in which the bentonite was collected from local sources. The Na-bentonite was firstly prepared before proceeding to cellulose embedment. The resultant B/Cell was characterized for its functional groups, morphology, and crystallinity. The Cr(VI) adsorption capacity and removal efficiency were determined based on batch adsorption. Our findings revealed that the B/Cell composite with a 4:1 bentonite-to-cellulose mass ratio exhibited the highest removal efficiency (85.68%) among tested formulations. Fourier-transform infrared spectroscopy, scanning electron microscopy, and X-ray diffraction analyses confirmed the successful integration of cellulose and structural modification of bentonite. Optimal adsorption was achieved at pH 3, 180-min contact time, and 10 g/L adsorbent dosage. Isotherm modeling showed excellent fits for Sips (R^2 = 0.9992) model, with maximum adsorption capacity reaching 192.56 mg/g. Kinetic analysis indicated pseudo-second-order kinetics (R^2 = 0.959, q_e = 1.018 mg/g), suggesting a chemisorption mechanism. These results highlight the potential of the B/Cell composite as an efficient and low-cost adsorbent for Cr(VI) removal from aqueous environments.

Keywords: adsorption, bentonite, cellulose, Freundlich, montmorillonite

1. INTRODUCTION

With heightened industrial activities, pollution of heavy metals, including chromium (Cr), has become a globally environmental concern [1]. Cr (VI) is the most common form of Cr found in the environment [2]. The concentration of Cr in the environment can be widely varied. A study of an ultramafic environment in Greece revealed that groundwater Cr concentrations ranged from 0.5 to 131.5 µg/L, exceeding the safety limit for drinking water [3]. In an area impacted by heavy traffic, Cr concentrations in various sources of water could range from 0.04 to 2.23 mg/kg [4]. In a leather tanning industrial region of South India, groundwater concentrations ranged from 0.01 to 0.19 mg/L, with 66% of samples surpassing the safety threshold [5]. This is concerning since this metal could adversely impact various organisms, including humans [6][7]. In the aquatic environment, chromium can bioaccumulate, posing a potential threat to the organisms or even human through food chain [8][9]. Contaminated environment heavily impact women, particularly because of the carcinogenicity of the heavy metal [9][10].

Bentonite, particularly when modified as organoclay, has been shown to be a reliable adsorbent for treating Cr(VI) in water [11][12]. A study reported organo-bentonite had a high adsorption capacity for Cr(VI), with optimal conditions at a pH of 3.4 and an adsorbent amount of 0.44 g, yielding a maximum adsorption capacity of 10.04 mg/g [13]. Following an optimization, magnetic bentonite was reported to exhibit nearly complete removal of Cr(VI), reaching 98.89% removal at a 6 mg/L concentration [14]. This potential can be improved by embedding biopolymers onto the clay surface. On the other hand, cellulose is a biopolymer that is not only highly abundant in nature, but also possesses high adsorption capacity against various heavy metal [15][16]. Therefore, the present study aimed to prepare a composite based on cellulose and bentonite. Previous studies reported that embedding cellulose increased Cr(III) removal efficiency by 5.0–6.5% compared to non-modified organoclay

Table 1. Composition variations of bentonite and cellulose in the preparation of B/Cell composite.

Label	Bentonite (g)	Cellulose (g)	Composition (%)	
			Bentonite	Cellulose
Bentonite	5	0	100	0
Cellulose	0	5	0	100
B/Cell 4:1	4	1	80	20
B/Cell 3:2	3	2	60	40
B/Cell 2:3	2	3	40	60
B/Cell 1:4	1	4	20	80

Figure 1. Photographed images of (a) Na-Bentonite, (b) cellulose, and B/Cell with compositions of (c) 1:4, (d) 2:3, (e) 3:2, and (f) 4:1.

[17]. In another study, interlayer modification of bentonite using cellulose resulted in effective removal of hazardous dye contaminants (maximum adsorption capacity of 140.85 mg/g) [18]. However, most existing studies focused either on Cr(III) or organic contaminants, and limited attention has been given to the application of cellulose-bentonite composites for Cr(VI) removal. Furthermore, Indonesian natural bentonite—despite being locally abundant—remains underutilized in biopolymer-based composite development. To address this gap, the present study aims to prepare and characterize a cellulose–bentonite composite using Indonesian bentonite for the efficient adsorption of Cr(VI).

2. MATERIALS AND METHODS

2.1. Materials

Materials used in this study were natural bentonite, alpha-cellulose, $K_2Cr_2O_7$, 1,5-diphenylcarbazide, NaCl 1 M, $AgNO_3$, H_2SO_4, ethanol, acetone, deionized water, HCl 0.1 M and NaOH 0.1 M. Otherwise specifically described, all materials were procured from Merck (Selangor, Malaysia) with analytical standard quality. Natural bentonite was collected Aceh Utara Regency, Aceh, Indonesia.

2.2. Preparation of Na-bentonite

Upon collection, bentonite in a powder form was rinsed with deionized water and dried in an oven (105 °C; 5 h). Thereafter, the bentonite (50 g) was added into a Beaker glass containing 500 mL NaCl 1 M, and subsequently stirred for 24 h at room temperature (25±1 °C). The formed precipitate was washed using deionized water until the chloride ion was completely removed. The bentonite paste was then dried in an oven (105 °C) for 24 h, and further

crushed and sieved (100 mesh) to obtain Na-bentonite fine powder.

2.3. Preparation of Bentonite/Cellulose

Composite B/Cell was prepared by mixing Na-bentonite and cellulose powders with varied concentrations in 100 mL deionized water as presented in Table 1. After being stirred for 24 h at 220 rpm and room temperature (25±1 °C), the composite was sequentially collected, oven-dried (105 °C, 24 h), and crushed to obtain the fine powder.

2.4. Characterization

Composite B/Cell was characterized using Fourier transform infrared (FT-IR) Prestige 21 (Shimadzu, Kyoto, Japan), where the infrared absorption observation was performed from 4000 to 500 cm^{-1}. We also employed Shimadzu XRD- 700 (Kyoto, Japan) to investigate the crystalline characteristics of the resultant composite. The scanning was carried out from 2θ = 10° to 80° at a rate of 2°/min using Cu Kα radiation generated by an X-ray tube operating at 40 kV and 30 mA. Moreover, the surface morphology of the resultant

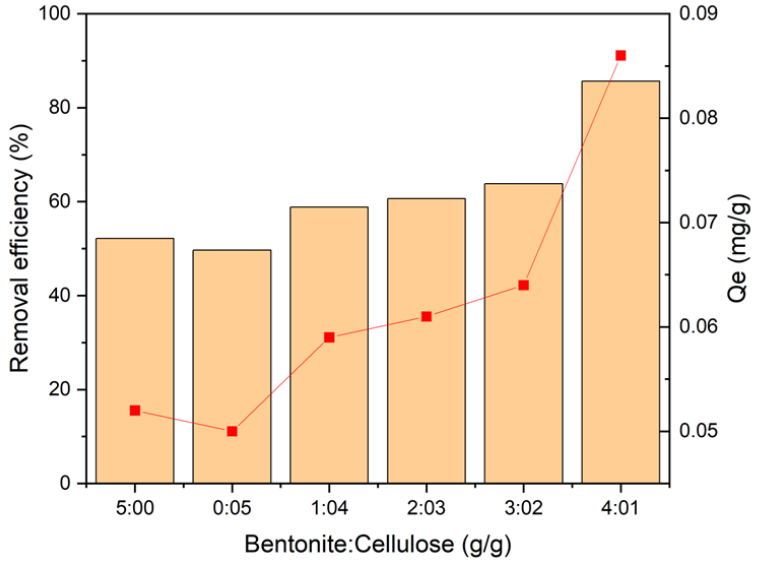

Figure 2. Effect of bentonite and cellulose compositions on the adsorptive removal of Cr(VI) by composite B/Cell.

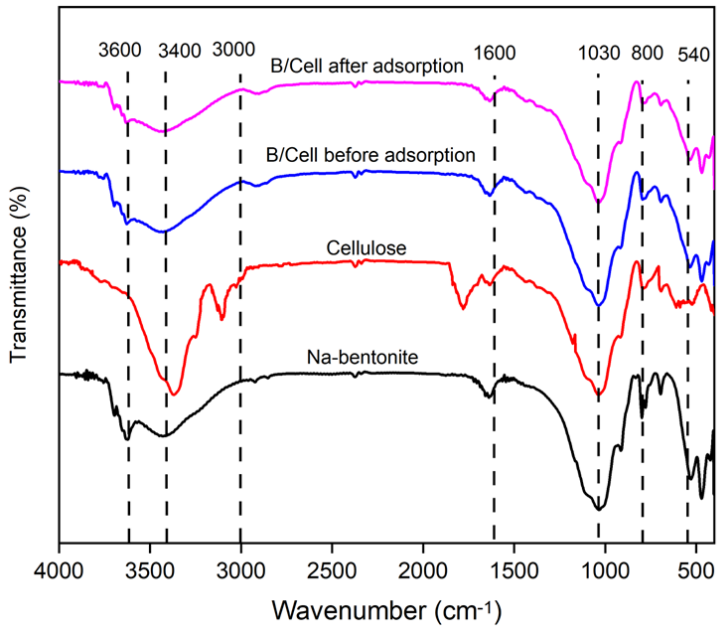

Figure 3. FT-IR spectra of Na-bentonite, cellulose, and B/Cell before and after used in Cr(VI) adsorption.

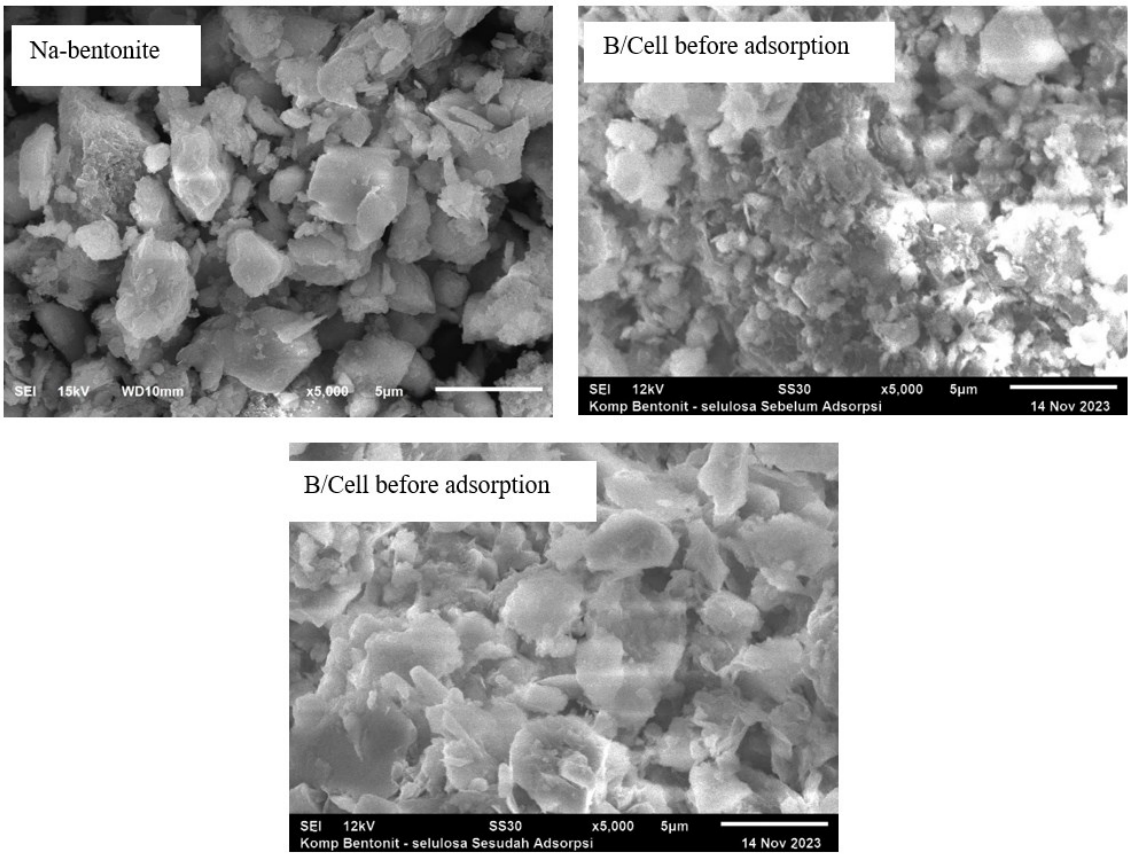

Figure 4. SEM images of Na-bentonite and composites B/Cell before and after used in Cr(VI) adsorption.

adsorbent was investigated through images generated by scanning electron microscope (SEM) Jeol. Jsm-6510 LA (Tokyo, Japan). SEM analysis was carried out at 12 kV under 5,000× magnification.

2.5. Batch Adsorption

Batch adsorption was carried out on Cr(VI) 25 mg/L with a volume of 20 mL (neutral pH). Upon the addition of adsorbent into the Cr(VI) solution, the container was sealed with aluminum foil and stirred at 200 rpm at 25 °C. To observe the effect of contact time, the batch adsorption was carried for 30 to 300 min with 30 min interval with Cr(VI) initial concentration of 25 mg/L and pH 7.7. To observe the effect of initial pH, the batch adsorption was carried on Cr(VI) 25 mg/L for 3 h with pH variation from pH 1 to pH 8. Adjustment of the initial pH was carried out by the drop-wising HNO_3 and KOH to decrease and increase the pH level, respectively. Effect of adsorbent mass was investigated by varying the adsorbent weight from 0.1 to 0.5 g with 0.1 g interval, where the initial concentration, pH, as well as contact time were set at 25 mg/L, pH 3, and 180 min. The adsorption isotherm was constructed based on the variation of initial Cr (VI) concentrations (25 to 125 mg/L), performed under optimum operating conditions. After the batch adsorption, the filtrate was collected and adjusted with 5 drops of H_3PO_4 and H_2SO_4 6 M, respectively, until the pH reached 2. Subsequently, the solution was added with deionized water (50 mL) and complexing agent 1,5-diphenylcarbadzide 4×10^{-3} M (0.2 mL). The remaining Cr(VI) concentration following the adsorption was calculated based on the absorbance at 566 nm using a UV-vis spectrophotometer (Uvmini-1240, Shimadzu, Kyoto, Japan). Each adsorption batch was performed in triplicate, where the data are presented as mean±standard deviation. Isotherm and kinetic modelings were carried out on Rstudio version 4.4.1 (Posit, PBC, Boston, MA, USA).

3. RESULTS AND DISCUSSIONS

3.1. Optimum Composition

The resultant composites and its raw materials are presented in Figure 1. Natural bentonite is

expected to contain rich Ca^{2+} that is likely to show non-swelling property. To ease the introduction of cellulose into the bentonite structure, hence, Ca^{2+} should be replaced with other ions such as Na^{+}. The introduction of cellulose, further resulted in the dark coloration of the adsorbent which could qualitatively indicate the presence of cellulose. In the present study, the preparation of B/Cell composite undergo a low temperature process. This is in accordance with previous study that did not involve heating process in preparation of bio-polymer-clay composites, and found efficient adsorption of Cr(VI) of more than 80% [19][20].

Effect of raw material compositions of B/Cell composites on Cr(VI) removal is presented in Figure 2. Sharp increase of adsorption capacity or removal efficiency was observed on B/Cell composite with bentonite:cellulose ratio of 4:1. The adsorption capacity as well as removal efficiency of aqueous Cr(VI) by B/Cell 4:1 were 0.085 mg/g and 85.68%, respectively. When compared with the neat bentonite, the removal efficiency increased by 33.5%. In previous studies, combination of bio-polymer chitosan and bentonite resulted similar adsorptive removal efficiency of over 80% [21] [22]. Increase of adsorption capacity of cellulose-based clay composites on various pollutant removals was also reported by previous studies [23] -[25]. Significant increase at a ratio where bentonite was four times higher than cellulose content is probably due to the blockage of the bentonite crystalline region by the cellulose molecules [26]. Since it showed the most optimum adsorption, the following investigations were performed on composite B/Cell 4:1.

3.2. FT-IR

FT-IR spectra of Na-bentonite, cellulose, along with B/Cell before and after used as adsorbent are presented in Figure 3. At a wavenumber range of 3600−3000 cm^{-1}, assigned for stretching vibration of O–H, the band was broader when the cellulose was embedded. The broadening of the spectral band is an indication of the hydrogen interaction involving the O–H moieties [27][28]. Typical IR spectral peaks of bentonite was observed at around 790, 530, and 1030 cm^{-1} which were assigned to Al (Mg)OH bond, Si–O–Al bond, and stretching Si–O –Si, respectively. Taken altogether, the embedment of cellulose onto Na-bentonite involved hydrogen interaction. Moreover, IR spectra of the B/Cell after the adsorption showed no vibration of Cr(VI) complex bonds. This suggests that the adsorption of Cr(VI) on the composite surface was dependent on electrostatic force [29].

3.3. SEM

SEM images of the Na-bentonite, as well as B/Cell before and after being used for Cr(VI) adsorption are presented in Figure 4. Sharp-particle

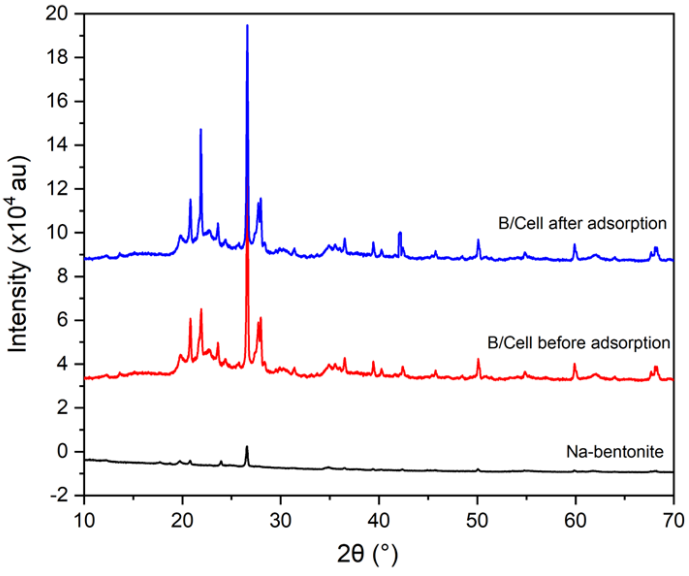

Figure 5. XRD diffractogram of Na-bentonite and composites B/Cell before and after used in Cr(VI) adsorption.

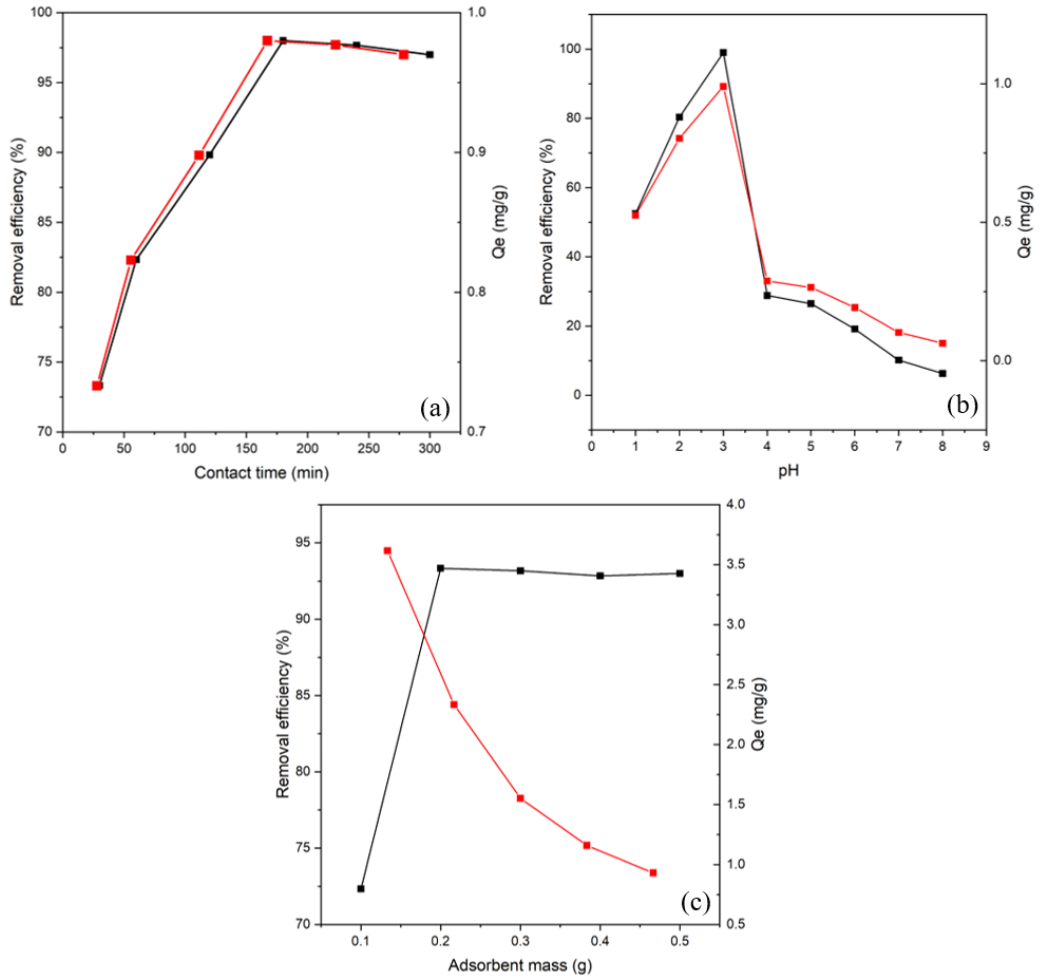

Figure 6. Effects of (a) contact time, (b) initial pH, and (c) adsorbent mass on the adsorptive removal of Cr(VI).

like was observed for Na-bentonite. Such structure is common for mineral morphology [30][31]. Following the cellulose introduction, a bulkier surface was observed, corroborating our speculation on the role of cellulose in blocking the bentonite structure. When the SEM images were taken on the adsorbent after the batch adsorption, the structure was observed to be swollen which was the characteristic of Na-bentonite and cellulose. The swelling is favored when it comes to adsorption in aqueous media as it allows more adsorbate to reach the binding sites [29][32].

3.4. XRD

XRD characteristics were observed for the Na-bentontie and composite B/Cell, where the diffractograms are presented in Figure 5. Predominant crystalline peaks were observed at 2θ = 21.91°, 26.61°, and 27.66° in Na-bentonite diffractogram, suggesting the characteristics of montmorillonite. This finding is similar with a previous study on the natural product, where they found high proportion of montmorillonite in bentonite [33]. Herein, crystalline peaks at 2θ = 20.82°, 21.91°, 23.61°, and 26.61° were observed in B/Cell diffractogram. Increases in peak intensity were observed in multiple peaks including (2θ = 20.82°, 21.91°, 23.61°, and 26.61°). Increase in peak intensity indicated the rearrangement of crystalline structure following the introduction of cellulose. This rearrangement is characterized by the expansion of the interlayer spacing, which is attributed to the exchange of Na^+ ions in the clay galleries with the positively charged cellulose [27][34].

3.5. Determining the Best Operating Parameter

The effects of operating parameter variations on Cr(VI) adsorption onto the B/Cell composite are presented in Figure 6. The highest adsorption was

obtained after 180 min adsorption. Shorter or longer contact time results in slightly lower adsorption. Initially (usually during the first 1 min of observation), the adsorption was driven by physical force, such as diffusion and other water-adsorbent interactions. This phase was not observed in our study, since the observation started at 30 min. Reduced adsorption observed afterward (>180 min) was thought to be derived from the leachate, as the adsorbate had formed layers distant from the adsorbent active sites. We further observed the highest adsorption at initial pH 3, where the lowest adsorption was found in basic pH range (pH 7−8). At pH 3, the removal efficiency reached 99% with adsorption capacity of 0.99 mg/g. High adsorptive removal at acidic pH range, was suspectedly caused by the negative speciation of Cr(VI) into $HCrO_4^-$ and $Cr_2O_7^{2-}$. Since the bentonite, cellulose, and its combination had positively charged survey, the electrostatic attraction favored adsorption of negatively charged ions (in this case are into $HCrO_4^-$ and $Cr_2O_7^{2-}$). Increase in pH level could alter the

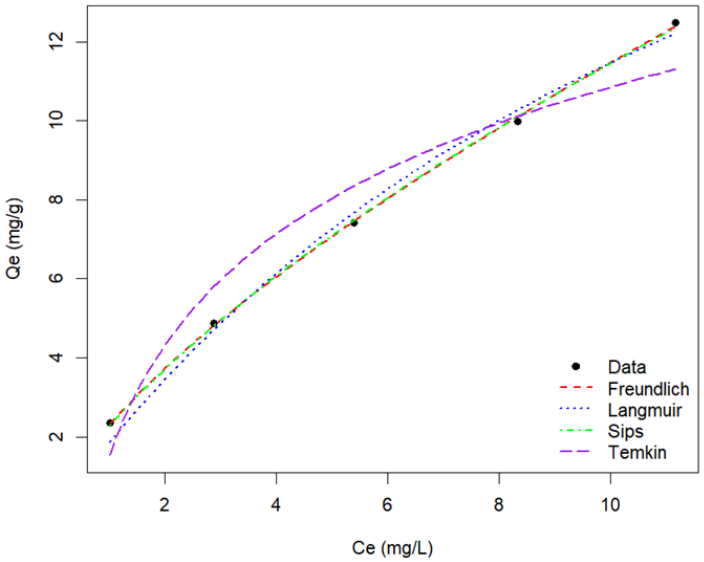

Figure 7. Freundlich, Langmuir, Sips, and Temkin fitting curves of the Cr(VI) adsorption onto B/Cell.

Table 2. Estimation of isotherm parameter of composite B/Cell for Cr (VI) adsorption.

Isotherm model	Parameter	Estimated value
Freundlich	K_F	2.305 mg/g
$q_e = K_F C_e^{1/n}{}_e$	n	1.435
	R^2	0.9995
Langmuir	Q_m	27.154 mg/g
$q_e = \frac{Q_m K_L C_e}{1 + K_L C_e}$	K_L	0.073 L/mg
	R^2	0.9921
Sips	Q_{ms}	192.560 mg/g
$q_e = \frac{Q_{ms} K_s C_e^{ns}}{1 + K_s C_e^{ns}}$	K_S	0.012 L/mg
	n_S	0.725
	R^2	0.9992
Temkin	B	4.056
$q_e = B \times Ln(AC_e)$	A	1.452
	R^2	0.9406

Note: K_F, Freundlich isotherm constant; n, Freundlich adsorption intensity; Q_m, Langmuir maximum adsorption capacity; K_L, Langmuir isotherm constant; Qms Sips maximum adsorption capacity; K_S, Sips isotherm constant; n_S, Sips heterogeneity factor; B, related to heat adsorption (J/mol); A, Temkin binding constant (L/g).

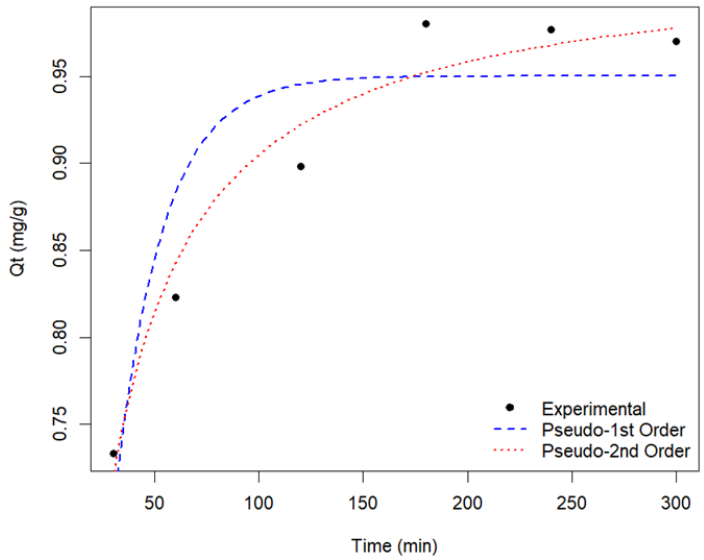

Figure 8. Pesudo-first-order and pseudo-second-order kinetic fitting curves of the Cr(VI) adsorption onto B/Cell.

Table 3. Estimation of kinetic parameters of composite B/Cell for Cr (VI) adsorption.

Kinetic Model	Parameter	Estimated Value
Pesudo-first-order	q_e	0.9501 mg/g
$q_t = q_e(1 - e^{-k_1 t})C_e^{1/n}{}_e$	k_1	0.044 min^{-1}
	R^2	0.8209
Langmuir	q_e	1.018 mg/g
$q_e = \frac{k_2 q_e^2 t}{1 + k_2 q_e^2 t}$	k_2	0.078 g/mg.min
	R^2	0.9590

Note: k_1, rate constant of pseudo-first-order; k_2, rate constant of second-order; t, contact time.

adsorbate to have positive charge, thus resulting in electrostatic repulsion with the adsorbent.

Mass of adsorbent was observed to affect the adsorption of Cr(VI), where the removal efficiency and adsorption capacity is expected to have inverse correlation. A removal efficiency of 93.33% was reached, when 0.2 g composite B/Cell (equivalent to 10 g/L) was used. Higher adsorbent mass was likely to result in decreased the adsorption, particularly when the adsorption capacity was observed. Effect of adsorbent mass could be explained by the density of absorbate in the aqueous media, where lower density resulted in reduced diffusion. The more the adsorbent added, the smaller the adsorbate density following the effective removal. In comparison with a previous study, Cr(III) reached optimal adsorption with adsorbent mass of 7 g/L and contact time of 90 min [35]. Taken altogether, the most efficient removal was reached when the contact time, initial pH, and adsorbent mass were 180 min, pH 3, and 10 g/L, respectively.

3.6. Adsorption Isotherm

The adsorption behavior of Cr(VI) was initially modeled using two-parameter isotherm models, namely Langmuir and Freundlich. The fitting curves are presented in Figure 7 and the estimated isotherm parameters are presented in Table 2. The Langmuir model yielded a high maximum adsorption capacity (Q_m = 27.154 mg/g) with strong correlation (R^2 = 0.9921), suggesting a favorable monolayer adsorption process. The Freundlich model provided an even better fit (R^2 = 0.9995), with K_F = 2.305 mg/g and n = 1.435, indicating multilayer adsorption with favorable intensity (n > 1), suggestive of chemosorption. Given the excellent fit of both models and the possibility of

heterogeneous surface interactions, we further applied the three-parameter Sips isotherm. This model demonstrated the highest adsorption capacity (Q_{ms} = 192.560 mg/g) and maintained a very good fit (R^2 = 0.9992), supporting a hybrid mechanism combining features of both Langmuir and Freundlich models. The Temkin model, which assumes that the heat of adsorption decreases linearly with increasing surface coverage due to adsorbate–adsorbent interactions, showed a relatively lower fit (R^2 = 0.9406), with B = 4.056 and A = 1.452. This suggests that while such interactions may be present, they play a less dominant role compared to the surface heterogeneity and capacity effects captured by the Sips model. Overall, the Sips model best described the Cr(VI) adsorption process, accounting for both monolayer and heterogeneous adsorption characteristics.

Similar to a previous study, the modified bentonite adsorbent had a higher likelihood to follow the Freundlich than the Langmuir assumptions, while the best fitness was observed in the Sips isotherm model [11]. Our data are also in line with adsorptive removals of heavy metals (Co and Cd) using Slovak bentonites that follows Sips model with n_S of less than 1 [36]. In comparison with another adsorbent such as magnetic graphene, the Q_{ms} only reached 5.17 mg/g in removing Cr(VI), suggesting the superiority of our newly developed Indonesian organoclay [37]. In previous research, however, only Freundlich-like adsorptive behavior of Cr(VI) onto bentonite was observed [38][39].

3.7. Adsorption Kinetics

The adsorption kinetics of Cr(VI) were evaluated using pseudo-first-order and pseudo-second-order models. The fitting curves are presented in Figure 8, and the estimation results are summarized in Table 3. The pseudo-first-order model showed a moderate fit (R^2 = 0.8209), with an equilibrium adsorption capacity (q_e) of 0.9501 mg/g and a rate constant (k_1) of 0.044 min^{-1}, indicating that this model may not fully capture the underlying mechanism, especially during the initial phase of adsorption. In contrast, the pseudo-second-order model exhibited a better fit to the experimental data (R^2 = 0.959), with a q_e of 1.018 mg/g and a rate constant (k_2) of 0.078 g/mg·min. This stronger correlation suggests that the adsorption process is primarily governed by chemisorption, involving electron sharing or exchange between Cr(VI) ions and active sites on the adsorbent. This interpretation is further supported by the Freundlich adsorption intensity value (n = 1.435), which is greater than 1, confirming the favorable and chemical nature of the adsorption.

In a reported investigation on the Slovak bentonite, the pseudo-second-order kinetic shows higher compability than that of pseudo-first-order [36]. Similarly, a published study reported a pseudo -second-order kinetic model as the best fit for Cr (VI) adsorption onto a graphen oxide nanohybrids (R^2 = 0.994–0.999), with higher adsorption capacities (q_e up to 7.45 mg/g) [40]. Furthermore, a study employing an anion exchange resin-based adsorbent, reported q_e = 0.805 mg/g and k_2 = 0.031 g/mg·min for Cr(VI) at pH 3, with R^2 of 0.989 under pseudo-second-order kinetics [41]. A similar trend was observed in another study using a PEI-functionalized magnetic Zr-MOF composite, where Cr(VI) adsorption reached equilibrium within 30 minutes and followed the pseudo-second-order model with high correlation (R^2 > 0.99) [42]. Although the adsorption capacity in the present study is relatively lower as compared to previous studies [40]-[42], the rate constant observed (k_2 = 0.078 g/mg·min) suggests a faster uptake than many nanocomposites, making it promising for short contact-time applications.

4. CONCLUSIONS

Composite B/Cell was prepared by embedding cellulose onto bentonite resulting in alteration of bentonite crystalline structure, morphology, and surface charge. Such changes benefit the adsorbent function to entrap Cr(VI), resulting in effective removal from the aqueous media. A Cr(VI) removal efficiency of over 90% obtained when the operating conditions were set at 180-min contact time, initial pH 3, and adsorbent mass of 0.2 g. Isotherm and kinetic analyses suggest that Cr(VI) adsorption onto the composite occurs through a heterogeneous multilayer process involving chemisorption at the active sites of the composite surface. In conclusion, the adsorbent has the potential for wastewater management, particularly in removing Cr(VI).

These findings suggest that the composite shows promise for practical wastewater treatment applications. However, further studies are needed to evaluate its regeneration capacity, reusability across multiple cycles, and performance under real industrial wastewater conditions. In addition, assessing the feasibility of large-scale production and operational challenges—such as handling, stability, and integration with existing treatment systems—will be essential. Future research should also explore combining this composite with other treatment technologies (e.g., filtration or advanced oxidation) to enhance overall treatment efficiency and cost-effectiveness.

AUTHOR INFORMATION

Corresponding Author

Julinawati Julinawati — Department of Chemistry, Universitas Syiah Kuala, Banda Aceh-23111 (Indonesia);
orcid.org/0009-0000-1945-9805
Email: julinawati@usk.ac.id

Authors

Eka Nadia — Department of Chemistry, Universitas Syiah Kuala, Banda Aceh-23111 (Indonesia);
orcid.org/0009-0008-6185-4364

Irfan Mustafa — Department of Chemistry, Universitas Syiah Kuala, Banda Aceh-23111 (Indonesia);
orcid.org/0000-0003-2283-4770

Suryati Suryati — Chemical Engineering Department, Universitas Malikussaleh, Lhokseumawe–24351 (Indonesia);
orcid.org/0000-0003-4089-8073

Author Contributions

Conceptualization, J. J. and I. M.; Methodology, Software, Resources, Original Draft Preparation, Visualization, Project Administration, J. J.; Validation, I. M. and S. S.; Formal Analysis, J. J., I. M., and S.S .; Investigation, Data Curation, E. N.; Writing –Writing – Review & Editing, E. N., I. M., and S. S.

Conflicts of Interest

The authors declare no conflict of interest.

REFERENCES

[1] J. J. Coetzee, N. Bansal, and E. M. N. Chirwa. (2018). "Chromium in Environment, Its Toxic Effect from Chromite-Mining and Ferrochrome Industries, and Its Possible Bioremediation". *Exposure and Health.* **12** (1): 51-62. 10.1007/s12403-018-0284-z.

[2] J. Liang, X. Huang, J. Yan, Y. Li, Z. Zhao, Y. Liu, J. Ye, and Y. Wei. (2021). "A review of the formation of Cr(VI) via Cr(III) oxidation in soils and groundwater". *Science of The Total Environment.* **774**. 10.1016/j.scitotenv.2021.145762.

[3] E. Vasileiou, P. Papazotos, D. Dimitrakopoulos, and M. Perraki. (2021). "Hydrogeochemical Processes and Natural Background Levels of Chromium in an Ultramafic Environment. The Case Study of Vermio Mountain, Western Macedonia, Greece". *Water.* **13** (20). 10.3390/w13202809.

[4] T. Ahmad, K. Ahmad, Z. I. Khan, Z. Munir, A. Khalofah, R. N. Al-Qthanin, M. S. Alsubeie, S. Alamri, M. Hashem, S. Farooq, M. M. Maqbool, S. Hashim, and Y. F. Wang. (2021). "Chromium accumulation in soil, water and forage samples in automobile emission area". *Saudi Journal of Biological Sciences.* **28** (6): 3517-3522. 10.1016/j.sjbs.2021.03.020.

[5] D. Karunanidhi, P. Aravinthasamy, T. Subramani, D. Kumar, and G. Venkatesan. (2021). "Chromium contamination in groundwater and Sobol sensitivity model based human health risk evaluation from leather tanning industrial region of South India". *Environmental Research.* **199** : 111238. 10.1016/j.envres.2021.111238.

[6] S. Prasad, K. K. Yadav, S. Kumar, N. Gupta, M. M. S. Cabral-Pinto, S. Rezania, N. Radwan, and J. Alam. (2021). "Chromium contamination and effect on environmental health and its remediation: A sustainable approaches". *Journal of Environmental Management.* **285** : 112174. 10.1016/j.jenvman.2021.112174.

[7] G. Gorbi, M. Invidia, C. Zanni, A. Torelli, and M. G. Corradi. (2004). "Bioavailability,

bioaccumulation and tolerance of chromium: consequences in the food chain of freshwater ecosystems". *Annales de Chimie.* **94** (7-8): 505-13. 10.1002/adic.200490064.

[8] K. Ahmad, M. Iqhrammullah, D. R. Rizki, A. Aulia, A. Q. Mairizal, A. Purnama, I. Qanita, S. N. Abdulmadjid, and K. Puspita. (2022). "Heavy Metal Contamination in Aquatic and Terrestrial Animals Resulted from Anthropogenic Activities in Indonesia: A Review". *Asian Journal of Water, Environment and Pollution.* **19** (4): 1-8. 10.3233/ajw220049.

[9] Y. Pratama, M. Kadir, A. Rivaldi, I. Mulya, S. Amirah, and M. Iqhrammullah. (2024). "Bibliometric analysis of the impact of environmental degradation on women and the importance of women's representation". *Global Journal of Environmental Science and Management.*

[10] M. Iqhrammullah, R. Y. Refin, R. I. Rasmi, F. F. Andika, H. Hajjah, M. Marlina, and R. Ningsih. (2023). "Cancer in Indonesia: A bibliometric surveillance". *Narra X.* **1** (2). 10.52225/narrax.v1i2.86.

[11] J. Julinawati, F. Febriani, I. Mustafa, F. Fathurrahmi, R. Rahmi, S. Sheilatina, K. Ahmad, K. Puspita, and M. Iqhrammullah. (2023). "Tryptophan-Based Organoclay for Aqueous Naphthol Blue Black Removal – Preparation, Characterization, and Batch Adsorption Studies". *Journal of Ecological Engineering.* **24** (7): 274-284. 10.12911/22998993/165781.

[12] K. Ahmad and W. Chiari. (2023). "Metal oxide/chitosan composite for organic pollutants removal: A comprehensive review with bibliometric analysis". *Narra X.* **1** (2). 10.52225/narrax.v1i2.91.

[13] J. D. Castro-Castro, I. F. Macias-Quiroga, G. I. Giraldo-Gomez, and N. R. Sanabria-Gonzalez. (2020). "Adsorption of Cr(VI) in Aqueous Solution Using a Surfactant-Modified Bentonite". *ScientificWorldJournal.* **2020** : 3628163. 10.1155/2020/3628163.

[14] G. Lemessa, Y. Chebude, and E. Alemayehu. (2023). "Adsorptive removal of Cr (VI) from wastewater using magnetite–diatomite nanocomposite". *AQUA — Water Infrastructure, Ecosystems and Society.* **72** (12): 2239-2261. 10.2166/aqua.2023.132.

[15] A. Rahman, K. Yoshida, M. M. Islam, and G. Kobayashi. (2023). "Investigation of Efficient Adsorption of Toxic Heavy Metals (Chromium, Lead, Cadmium) from Aquatic Environment Using Orange Peel Cellulose as Adsorbent". *Sustainability.* **15** (5). 10.3390/su15054470.

[16] Q. Wu, H. He, H. Zhou, F. Xue, H. Zhu, S. Zhou, L. Wang, and S. Wang. (2020). "Multiple active sites cellulose-based adsorbent for the removal of low-level Cu (II), Pb(II) and Cr(VI) via multiple cooperative mechanisms". *Carbohydrate Polymers.* **233** : 115860. 10.1016/j.carbpol.2020.115860.

[17] C. Soloviy, M. Malovanyy, O. Palamarchuk, I. Trach, H. Petruk, H. Sakalova, T. Vasylinych, and N. Vronska. (2021). "Adsorption method of purification of stocks from chromium(III) ions by bentonite clays". *Journal of Water and Land Development.* 99-104. 10.24425/jwld.2021.136152.

[18] S. J. Priatna, Y. M. Hakim, S. Wibyan, S. Sailah, and R. Mohadi. (2023). "Interlayer Modification of West Java Natural Bentonite as Hazardous Dye Rhodamine B Adsorption". *Science and Technology Indonesia.* **8** (2): 160-169. 10.26554/sti.2023.8.2.160-169.

[19] A. L. Obsa, N. T. Shibeshi, E. Mulugeta, and G. A. Workeneh. (2024). "Bentonite/amino-functionalized cellulose composite as effective adsorbent for removal of lead: Kinetic and isotherm studies". *Results in Engineering.* **21**. 10.1016/j.rineng.2024.101756.

[20] J. Jia, Y. Liu, and S. Sun. (2021). "Preparation and Characterization of Chitosan/Bentonite Composites for Cr (VI) Removal from Aqueous Solutions". *Adsorption Science & Technology.* **2021** : 6681486. 10.1155/2021/6681486.

[21] Z. Deng, Z. Wu, Q. Wu, J. Yu, C. Zou, H. Deng, P. Jin, and D. Fang. (2024). "Cellulose nanocrystals intercalated clay biocomposite for rapid Cr(VI) removal". *Environmental*

Science and Pollution Research. **31** (20): 29719-29729. 10.1007/s11356-024-33066-7.

[22] J. Yang, B. Huang, and M. Lin. (2020). "Adsorption of Hexavalent Chromium from Aqueous Solution by a Chitosan/Bentonite Composite: Isotherm, Kinetics, and Thermodynamics Studies". *Journal of Chemical & Engineering Data.* **65** (5): 2751-2763. 10.1021/acs.jced.0c00085.

[23] R. Tang, Z. Wang, Y. Muhammad, H. Shi, K. Liu, J. Ji, Y. Zhu, Z. Tong, and H. Zhang. (2021). "Fabrication of carboxymethyl cellulose and chitosan modified Magnetic alkaline Ca-bentonite for the adsorption of hazardous doxycycline". *Colloids and Surfaces A: Physicochemical and Engineering Aspects.* **610**. 10.1016/j.colsurfa.2020.125730.

[24] R. D. Fan, K. R. Reddy, Y. L. Yang, and Y. J. Du. (2020). "Index Properties, Hydraulic Conductivity and Contaminant-Compatibility of CMC-Treated Sodium Activated Calcium Bentonite". *International Journal of Environmental Research and Public Health.* **17** (6). 10.3390/ijerph17061863.

[25] Y. Chen, Z. Nie, J. Gao, J. Wang, and M. Cai. (2021). "A novel adsorbent of bentonite modified chitosan-microcrystalline cellulose aerogel prepared by bidirectional regeneration strategy for Pb(II) removal". *Journal of Environmental Chemical Engineering.* **9** (4). 10.1016/j.jece.2021.105755.

[26] S. P. Santoso, A. Kurniawan, F. E. Soetaredjo, K.-C. Cheng, J. N. Putro, S. Ismadji, and Y.-H. Ju. (2019). "Eco-friendly cellulose–bentonite porous composite hydrogels for adsorptive removal of azo dye and soilless culture". *Cellulose.* **26** (5): 3339-3358. 10.1007/s10570-019-02314-2.

[27] S. Cukrowicz, B. Grabowska, K. Kaczmarska, A. Bobrowski, M. Sitarz, and B. Tyliszczak. (2020). "Structural Studies (FTIR, XRD) of Sodium Carboxymethyl Cellulose Modified Bentonite". *Archives of Foundry Engineering.* 119-125. 10.24425/afe.2020.133340.

[28] Z. Su, L. Yu, L. Cui, G. Zhou, X. Zhang, X. Qiu, C. Chen, and X. Wang. (2023). "Reconstruction of Cellulose Intermolecular Interactions from Hydrogen Bonds to Dynamic Covalent Networks Enables a Thermo-processable Cellulosic Plastic with Tunable Strength and Toughness". *ACS Nano.* **17** (21): 21420-21431. 10.1021/acsnano.3c06175.

[29] Rahmi, M. Iqhrammullah, U. Audina, H. Husin, and H. Fathana. (2021). "Adsorptive removal of Cd (II) using oil palm empty fruit bunch-based charcoal/chitosan-EDTA film composite". *Sustainable Chemistry and Pharmacy.* **21**. 10.1016/j.scp.2021.100449.

[30] Marlina, M. Iqhrammullah, S. Saleha, Fathurrahmi, F. P. Maulina, and R. Idroes. (2020). "Polyurethane film prepared from ball-milled algal polyol particle and activated carbon filler for NH(3)-N removal". *Heliyon.* **6** (8): e04590. 10.1016/j.heliyon.2020.e04590.

[31] T. A. Saleh, A. Sarı, and M. Tuzen. (2021). "Development and characterization of bentonite-gum arabic composite as novel highly-efficient adsorbent to remove thorium ions from aqueous media". *Cellulose.* **28** (16): 10321-10333. 10.1007/s10570-021-04158-1.

[32] R. Rahmi, L. Lelifajri, M. Iqbal, F. Fathurrahmi, J. Jalaluddin, R. Sembiring, M. Farida, and M. Iqhrammullah. (2022). "Preparation, Characterization and Adsorption Study of PEDGE-Cross-linked Magnetic Chitosan (PEDGE-MCh) Microspheres for Cd2+ Removal". *Arabian Journal for Science and Engineering.* **48** (1): 159-167. 10.1007/s13369-022-06786-6.

[33] M. Moersilah, A. Rahman, E. Alanas, Y. Yuliani, and R. Rosmalia. (2021). "Synthesis and characterization of composite magnetite-bentonite from Indonesian local minerals". *IOP Conference Series: Materials Science and Engineering.* **1098** (6). 10.1088/1757-899x/1098/6/062045.

[34] A. O. Akar, U. H. Yildiz, and U. Tayfun. (2021). "Investigations of polyamide nano-composites containing bentonite and organo-modified clays: Mechanical, thermal, structural and processing performances".

Reviews on Advanced Materials Science. **60** (1): 293-302. 10.1515/rams-2021-0025.

[35] L. Frolova and B. Blyuss. (2023). "Investigation of Cr(III) adsorption in aqueous solution using bentonite". *Applied Nanoscience.* **13** (7): 5323-5333. 10.1007/s13204-023-02767-9.

[36] M. Suranek, Z. Melichova, and M. Thomas. (2024). "Removal of cadmium and cobalt from water by Slovak bentonites: efficiency, isotherms, and kinetic study". *Environmental Science and Pollution Research.* **31** (20): 29199-29217. 10.1007/s11356-024-33133-z.

[37] Ngainunsiami, Lalhmunsiama, and D. Tiwari. (2025). "Facile synthesis of novel graphene-based magnetized nanocomposite for the simultaneous elimination of lead (II) and chromium (VI) in aqueous medium: Insights of interfacial studies". *Chemical Engineering Research and Design.* **219** : 67-78. 10.1016/j.cherd.2025.05.056.

[38] A. Ahmadi, R. Foroutan, H. Esmaeili, and S. Tamjidi. (2020). "The role of bentonite clay and bentonite clay@MnFe2O4 composite and their physico-chemical properties on the removal of Cr(III) and Cr(VI) from aqueous media". *Environmental Science and Pollution Research.* **27** (12): 14044-14057. 10.1007/s11356-020-07756-x.

[39] Z. Li, P. Zou, J. Yang, M. Huang, L. Zhang, C. Huang, F. Yang, R. Huang, S. Lv, and G. Wei. (2021). "A functionalized tannin-chitosan bentonite composite with superior adsorption capacity for Cr(VI)". *Journal of Polymer Engineering.* **41** (1): 34-43. 10.1515/polyeng-2020-0133.

[40] S. Singh, A. G. Anil, S. Khasnabis, V. Kumar, B. Nath, V. Adiga, T. S. S. Kumar Naik, S. Subramanian, V. Kumar, J. Singh, and P. C. Ramamurthy. (2022). "Sustainable removal of Cr(VI) using graphene oxide-zinc oxide nanohybrid: Adsorption kinetics, isotherms and thermodynamics". *Environmental Research.* **203** : 111891. 10.1016/j.envres.2021.111891.

[41] C. Marcu, V. Codruţa, and A. and Balla. (2021). "Adsorption Kinetics of Chromium (VI) from Aqueous Solution Using an Anion Exchange Resin". *Analytical Letters.* **54** (1-2): 140-149. 10.1080/00032719.2020.1731523.

[42] C. Wang, C. Xiong, Y. He, C. Yang, X. Li, J. Zheng, and S. Wang. (2021). "Facile preparation of magnetic Zr-MOF for adsorption of Pb(II) and Cr(VI) from water: Adsorption characteristics and mechanisms". *Chemical Engineering Journal.* **415**. 10.1016/j.cej.2021.128923.